ОБЪЕДИНЕННЫЙ
ИНСТИТУТ
ЯДЕРНЫХ
ИССЛЕДОВАНИЙ

Дубна

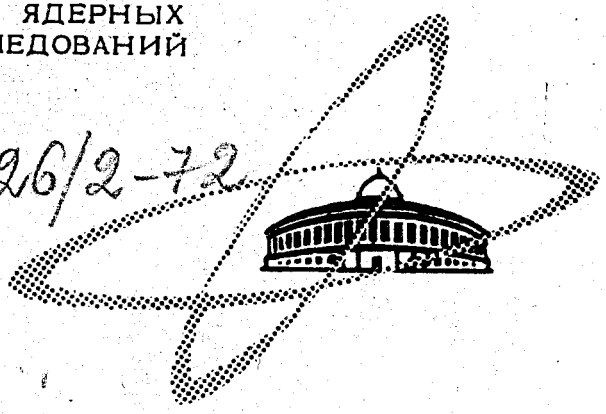

E14 - 6266

H.Eschrig, P.Urwank, K.Feldmann, K.Hennig, L.Weiss

PHONONS IN $MgZn_2$: MODEL POTENTIAL CALCULATIONS AND NEUTRON SCATTERING EXPERIMENTS

1972

E14 - 6266

H.Eschrig,[1] P.Urwank,[1] K.Feldmann, K.Hennig, L.Weiss[2]

PHONONS IN $MgZn_2$: MODEL POTENTIAL CALCULATIONS AND NEUTRON SCATTERING EXPERIMENTS

Submitted to V Symposium on Inelastic Neutron Scattering (Grenoble, France, March 6-10, 1972)

[1] Technical University of Dresden, GDR

[2] Central Institute for Nuclear Research, Rossendorf, GDR

Abstract

Model potential theory is used to calculate the dispersion curves, the photon density of states and the pressure (temperature) dependence of some phonon frequencies in the Laves phase $MgZn_2$. Since the elementary cell contains 12 atoms, the phonon spectrum is rather complicated. Nevertheless, there are very remarkable features of this spectrum, connected with low energy optical modes, the cagomee vibrations, which show soft mode behaviour. This may explain the singularities of the specific heat of $MgZn_2$ and $CaMg_2$ at low temperatures. Neutron scattering experiments have been carried out at the pulsed reactor in Dubna on polycrystalline samples for 300K at scattering angles 75, 90, 100, 110, 120° and for 90° at temperatures 77, 300, 853, 943, 1003K using the time-of-flight technique with the Be-filter in front of the detector. The obtained density of states and its temperature dependence are in good agreement with the theoretical predictions. This shows that the Shaw-model-potential-method is applicable even to such a complicated intermetallic compound as $MgZn_2$.

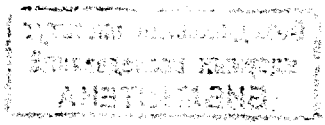

I. Introduction

The phonon spectra of pure metals widely experimentally and, in the case of non-transition metals, also theoretically have been studied in the past. It seems natural to extent these investigations to more complicated systems, as e.g. intermetallic compounds. In the present paper some results of both theoretical and experimental investigations of phonon spectra in the intermetallic compound $MgZn_2$ are given. $MgZn_2$ has the structure of one of the three Laves phases, commonly designated by C14. There is a large number of representatives of this structure type, but only very few, where both constituents are simple metals as is a necessary supposition of our theoretical pseudopotential treatment.

C14 structures show some remarkable physical properties. From the mechanical point of view they are very hard and brittle. Nevertheless, our investigations seem to show that there exist soft optical phonon modes in $MgZn_2$ and from structure considerations it is seen that this should be a general property of the C14 phase. The existence of soft phonon modes in the C14 phase also is stressed by specific heat measurements in the case of $CaMg_2$ /1/, XAl_2 where X stands for several rare earth metals /2/, and, very recently, also for $MgZn_2$ /3/. In all these cases a violation of Debye's T^3 law at comparatively low temperatures is found (remarkable increase of the lattice part of the specific heat above the T^3 curve from about $5K$ on). Moreover, at $10K$ and $16K$ the specific heat of $CaMg_2$ and $MgZn_2$, respectively, shows an anomaly, which looks like a second order phase transition /1,3/. There is a jump down in the specific heat curve as the temperature increases. It is known from other systems (e.g. V_3Si, which has β-W type structure /4/) that a low temperature second order lattice phase transition may be connected by a soft optical pho-

non mode. Since both substances $CaMg_2$ and $MgZn_2$ are non-magnetic and the superconductivity transition temperature is known to be much lower than 10K, the phase transition mentioned above may be expected also to be a lattice transition. So the existence of soft optical phonon modes in C14 structures also might fit this picture.

In the following section of this paper a more detailed discussion of the C14 structure is given. In section 3 results of a model potential calculation of phonon dispersion curves and of the phonon density of states of $MgZn_2$ are presented. The polarization vectors of some low lying modes are discussed. For zero wave-vector also the temperature and pressure dependence of the phonon frequencies is investigated and a lattice instability due to one soft optical phonon mode is found. Incoherent neutron scattering data for polycrystalline $MgZn_2$ samples are given in section 4 and comparison with the theoretical results is made. In section 5 the work is summarized.

2. Structure

The Wigner-Seitz cell of $MgZn_2$ is given in Fig. 1. There are eight zinc atoms per unit cell at positions

$$\underline{r}_1 = 0, \quad \underline{r}_2 = (0,0,c/2), \quad \underline{r}_3 = -\underline{r}_8 = (-3ax/4, \sqrt{3}ax/4, c/4),$$

$$\underline{r}_4 = -\underline{r}_7 = (0, -\sqrt{3}ax/2, c/4), \quad \underline{r}_5 = -\underline{r}_6 = (3ax/4, \sqrt{3}ax/4, c/4),$$

and four magnesium atoms at positions

$$\underline{r}_9 = (a/2, -a/(2\sqrt{3}), c(1-2z)/2), \quad \underline{r}_{10} = (a/2, -a/(2\sqrt{3}), cz),$$

$$\underline{r}_{11} = (a/2, a/(2\sqrt{3}), -cz), \quad \underline{r}_{12} = (a/2, a/(2\sqrt{3}), -c(1-2z)/2),$$

with

$$a = 9.856 \text{ a.u.}, \quad c = 16.184 \text{ a.u.}, \quad x = 1/3, \quad z = 1/16.$$

The corresponding Brillouin zone with the designation of points and lines used by us is given in Fig. 2. The structure has exactly the same symmetry as the common hcp structure. It is built by a special stacking sequence of close-packed lattice planes (planes of magnesium atoms and of zinc atoms 1 and 2, respectively) and of so-called cagomee planes (planes of zinc atoms 3,4,5 and 6,7,8, respectively).

For understanding of the vibrational behaviour discussed later on it is useful also to look at this structure from another point of view as shown in Fig. 1. The crystal consists of chains of double tetrahedrons of zinc atoms 2,3,4,5,1,6,7,8,13, the space between which is filled by dump-bells of magnetism atoms 11,12.

3. Model Potential Calculations

3.1. Method

The elements of the dynamical matrix are calculated using model potential theory in second order perturbation (see e.g. /5/). The energy-wave-number characteristic is computed from the non-local and energy depended Shaw potential /6/, where the core shifts are assumed to be the same as in the pure metals Mg and Zn, respectively. This assumption might be reasonable since Mg and Zn have the same valency and the mean atomic volume in $MgZn_2$ is nearly the same as in the pure metals Mg and Zn. The change of the core shift in alloying recently was studied /7/ and found to be small even in extremal cases.

Exchange and correlation effects are included into the energy-wave-number characteristic by a correction factor firstly suggested by Hubbard. We have proved our procedure to give reasonable results for phonon spectra for both pure Mg and Zn with this correction factor.

Because of the 12 atoms per unit cell, the dynamical matrix is a 36x36 matrix. Computing its elements summations are ranged over about 800 reciprocal lattice vectors. By a convergence test this is found to be sufficient for an 0.1 p.c. accuracy with exception of the very low lying branches, which are less accurate (5 p.c.).

The dynamical matrix and from this the phonon frequencies and polarization vectors are calculated at 870 equidistant points within the Brillouin zone. The Brillouin zone is divided into (non-regular) tetrahedrons the corners of which are these 870 points. The contribution of each tetrahedron to the density of states is calculated analytically by linear interpolating of the energy values at the corners. Then the contributions of all tetrahedrons are summed (see /8/ for the method).

3.2. Dispersion Curves

The calculated phonon dispersion curves for some symmetry lines are shown in Fig. 5. The connection of the branches is studied by group theoretical compatibility relations. We must say that there are some uncertainties in the connection of the branches of the upper part of the spectra on lines Σ and T. There are four symmetry types on these lines and therefore the branches are allowed to cross each other several times. In general, however, only the detailed dispersion relations of the lower energy of such a complicated excitation spectrum are of physical interest.

The most interesting feature of the lower part of the spectra, shown in Fig. 5, is the existence of extremely low lying optical branches. On the line Δ (hexagonal axis) there are four such branches in Fig. 3 denoted by Λ_3, Λ_4 and Λ_5 (twofold degenerated). As is shown from the calculated polarization vectors they belong to vibrations of the zinc double tetrahedrons as rigid structures. Two of them (Δ_3 and Λ_4) belong to rotational vibrations of the zinc double tetrahedrons around the c–c axis of Fig. 4, the magnesium atoms at the same time being in rest. At point Γ subsequent double tetrahedrons in c–c direction are in equal-phase for the Λ_3 mode and in antiphase for the Λ_4 mode. It is seen by group theoretical analysis that the polarization vectors of these two branches are completely determined, by the symmetry, independent of the interionic potential. (See /9/ for details of the symmetry properties of the spectra on Δ). Since the surrounding of a given chain of zinc double tetrahedrons has a high symmetry according to the c–c axis of Fig. 4, we believe that the soft-mode-character of these rotational vibrations also is a structural property independently of the interionic potential. That means, this feature of the spectra should be expected to be general for CI_4 type compounds and should be regarded as the cause of the anomalous low temperature behaviour of the specific heat of CI_4 structures.

The twofold degenerated Λ_5 branch belongs to a nodding vibration of the zinc double tetrahedrons around the a–a and b–b axis of Fig. 4, respectively. The magnetism dumb-bells nod only very slightly. All higher frequency modes are more or less connected with deformations of the zinc tetrahedrons.

3.3. Temperature and Pressure Dependence of the Frequencies at Γ

We have examined the behaviour of the phonon frequencies at point Γ with respect to a change of the density of the crystal in or-

der to study the effect of thermal expansion or pressure on the phonon dispersion. We are now especially interested in the low lying branches. As is already mentioned, the summation of the contribution of 800 reciprocal lattice vectors to the dynamical matrix is not sufficient for convergence in the case of low frequencies. Therefore, here we have summed up the contributions of 2100 reciprocal lattice vectors. The numerical error then is seen to be smaller than $2.10^{11} s^{-1}$ also for the lowest frequencies. The results are shown in Fig. 5. (The notation of the lowest frequencies corresponds to that of the lowest branches on Δ in Fig. 4. The difference in the frequency values of Fig. 4 and Fig. 5 are caused by the higher numerical exactness in Fig. 5). All frequencies behave quite normal with the exception of that of the Δ_3 branch, which becomes very weak in the low temperature (high pressure) limit. From this fact one can conclude that the system tends to a second order phase transition, where the normal co-ordinate of the Λ_3 phonon may be used as the order parameter. Since the actual zero of the Δ_3 frequency is rather sensitive to the special form of the used model potential, we don't believe that the calculation of the phase transition point is a reasonable task at the present stage of model potential theory. It may very likely be that it is just this phase transition, which causes the measured anomaly in the lattice specific heat of $MgZn_2$ and also of $CaMg_2$ /1,3/.

3.4. Density of States

The calculated density of states is seen in Fig. 6. It shows a many peaked structure due to the large number of interacting branches. One should expect that this curve would become smoothed out rigorously, if one would take into account line broadening due to the finite lifetime of the phonons. The low lying branches result in a broad peak in the low frequency range, which causes the unusual behaviour of the specific heat Debye temperature in the temperature range between 10K and 25K /3/.

4. Experiments

4.1. Apparatus

The measurements of the spectra of inelastically scattered neutron on $MgZn_2$ were performed on a time-of-flight spectrometer with a cooled beryllium filter in front of the detector (inverted geometry) /10/ at the pulsed reactor in Dubna /11/. The neutrons of the white beam are down scattered. For the energy analysis neutrons with a me-

an energy of 4.08 meV were used. The collimation is poor (0.2). The channel width of the time analyzer was 64 μsec. The flight path between moderator and sample was 20 or 31 m and between sample and detector 0.9 or 1.2 m, respectively. This gives an energy resolution (halfwidth of a very asymmetric function/12/) of about 15 to 8% for an energy transfer of 10 to 50 meV, respectively. With the spectrometer resolution function from /12/ we folded the theoretical phonon spectrum, Fig. 6, and obtained the broken curve.

The reactor was operated with the mean thermal power of 30 kW (pulse power of 150 MW), a pulse repetition rate of 5 pulses per second and a pulse width of about 100 μsec for thermal neutrons.

Highly purified $MgZn_2$ was used for preparing polycrystalline samples, plates 200 x 200 x 5 mm^3, which were studied at 77 and 300 K. Measurements on $MgZn_2$ at 853, 943 and 1003K were done within a Ta crucible 230 x 90 x 4 mm^3 which had a wall thickness of 0.2 mm. The temperature constance was better than $\pm$ 5K in all cases. At 300K measurements were carried out at different angles: 45, 60,75,90,100,110,120°; at the other temperatures the scattering angle was 90°. The scattered neutrons were counted for periods of about 24 hours followed by background counts for about 12 hours.

4.2. Experimental Results

In Fig. 7 are shown time-of-flight spectra measured at room temperature for scattering angles of 75,90,100,110,120° with a momentum transfer (Q) range of 1.9 to 5.3 A^{-1} and an energy transfer range of 5 to 40 meV. The channel width of the time analyzer was 64 μ sec, and the maximum of the Be cut-off appeared at N = 506. The flight path's were 31 and 1.2 m. These spectra were corrected for background, not for the reactor spectrum, and normalized to equal counting times. Moreover, the spectra were averaged over three neighbouring points. The error bars show the statistical errors and refer to the unaveraged data. All data handling calculations as well as theoretical ones have been made with the computers BESM-4 and BESM-6.

The data at 90° and backward angles of scattering were significantly more accurate than those at forward angles owing to the angular dependence of the inelastically scattered component and the larger solid angle subtended by the detectors.

Figure 8 shows the time-of-flight spectra for the scattering angle of 90° at temperatures 77,300,853,943 and 1003K. The melting point of $MgZn_2$ is 863K. The counting rate in the higher energy maxi-

mum is chosen to be nearly the same for all temperatures. The origins of the ordinates (arbitrary linear scale) of the different spectra are shifted relatively to each other.

The measurements at 853, 943 and 1003K were done with a shorter flight path from the reactor to the sample (20m) than in Fig. 7 (31m). Due to the heating facility and the smaller sample the measurements at temperatures higher than 300K are less accurate. The intensity of the 77K measurement for $N < 150$ is too large, due to the existence of very intensive satellites of fast neutrons at S.

4.3. Analysis and Discussion

The incoherent scattering amplitude of $MgZn_2$ for thermal neutrons is about 5% of the total scattering amplitude. In such a case it is possible to get some approximated information about the frequency distribution using the incoherent approximation, which is valid for high momentum transfer, extrapolating to zero-momentum transfer /13/. This is exact only for isotropically vibrating crystals. Unfortunately the extrapolation technique yields results with poor resolution as it involves interpolation between data points which have to be very accurate. Not only background effects but also multiple scattering may severely effect the result. Furthermore the lack of resolution is inherent in the extrapolation method /13,14/. In a single time-of-flight spectrum, especially for small Q, coherence effects can be pronounced and van Hove singularities may be observed if the instrumental resolution is good enough. There is no theory yet which gives an overall satisfying answer to these problems. It seems reasonable to suppose that the neutron data be used at one angle, preferable for large Q, to estimate the frequency distribution, since this procedure does give good agreement in many cases with frequency distributions calculated from dispersion curves, see /14/ p. 337 and /15/. We proved this on niobium comparing our results with these obtained from dispersion curves in /16/. The accuracy for peak positions and the cut-off frequency is much better than for intensities of the frequency distribution at different energies.

The aim of these scattering experiments on polycrystalline samples of $MgZn_2$ was to compare the experimental obtained cut-off frequency, the peak positions, and their temperature dependence with the theoretical phonon spectra calculated on the basis of pseudopotential parameters of the pure metals.

In Fig. 7 the position of the cut-off frequencies (I), as well as the positions of the maxima (2) and (3), are independent of the scattering angle. The change of intensity of the spectra fordifferent angles reflects the angular dependence ($\sim Q^2$) of one-phonon processes. The angular dependence of (4) and (5) seems to be a virtual one if we assume that the broad peak for 90 ^{o} (N = 330) has partly coherent character, which is diminishing with rising scattering angle. A more detailed comparison will be made during the discussion of Fig. 9.

The temperature dependence of the spectra of inelastically scattered neutrons, Fig. 8, shows a small shift of the maxima to lower energies and broadening of them with increasing temperature. At higher energies no remarkable change in the spectra measured on solid and liquid $MgZn_2$ is observed. This behaviour is connected with the temperature dependence of the $MgZn_2$ density and the short range order in liquid $MgZn_2$ and is in accordance with other results for instance /17/ . At lower energies (< 5 meV) the spectra are changing rapidly with increasing temperature so that already in the solid phase at 853K no Be cut-off is seen. We tried to estimate this large scattering amplitude for lower energies of liquid phase on the basis of the coherent scattering of Kadanov and Martin /18/ , the model of Vineyard /19/ and the population of phonon states. In the first and second case the sound velocity and the diffusion coefficient, respectively, differ by about one order from the known values. The estimation of the population gives more reasonable results. For more details see /20/. Therefore we believe that at high temperatures for solid $MgZn_2$ and the liquid phase the low lying cagomee vibrations, Fig.3, play a quite important role.

There is another proposal different from the extrapolation method for getting some information about the frequency distribution of materials mainly coherently scattering neutrons /21/ : One has to average over all Q vectors and over all polarizations of phonons. The polycrystalline sample quarantees the averaging over all polarizations and our poor collimation of the second flight path causes a certain averaging over a Q range $\Delta Q / Q$ = 0.1 to 0.07 for energy changes from 5 to 40 meV, respectively. Using some more or less rigorous assumptions: isotrop one atomic substance, approximated Debye-Weller factor /20/ and rotational symmetry distribution of the wave vectors of the ingoing and outgoing neutrons, we calculated for different scattering angles the frequency distribution function analogous to eq. (6) /17/ for downscattering. Using the experimental data from Fig. 7 and taking into account the reactor spectrum we get the

result plotted in Fig. 9. The line ftc is the folded theoretical curve from Fig. 6. The agreement between the experimental curves especially at 120 and the theoretical (ftc) is unexpectedly good. The cut-off frequencies $E_{(1)}^{exp} = (40 \pm 2) \cdot 10^{12}$ sec^{-1} and $E_{(1)}^{th} = (43.7 + 2) \cdot 10^{12}$ sec^{-1} and the positions of the main maxima (3) $E_{(3)}^{exp} = (27 \pm 2) \cdot 10^{12}$ sec^{-1} and $E_{(3)}^{th} = (27 \pm 2) \cdot 10^{12}$ sec^{-1} which are rather independent of the data handling procedure, see Fig. 7 and Fig. 9, show that the pseudopotential method is aplicable even to such complicated systems as the intermetallic compound $MgZn_2$. Peak (5) in Fig. 9 is mainly due to cagomee vibrations, compare Fig. 3. For more detailed information however measurements on single crystals are necessary.

Acknowledgement

We are grateful to Prof. G. Heber, Prof. P. Ziesche and Prof. G.E.R.Schulze(Technical University Dresden)for initiation and helpful discussions. We thank Prof. F.L. Shapiro and Dr. J. Ostanevich (Joint Institute for Nuclear Research) for their support. We are much in debt to Dr. I. Natkaniec (JINR) for experimental, Mr. K.-F. Hubner (JINR) for calculational assistance, and Dr. P.Paufler (TU) for the samples.

References

1. Davison J.E., Smith J.F. Transaction of the Metallurgical Society of AIME 242, 2051 (1968).
2. Hungsberg R.E., Gschneider K.A. Preprint 2887, Aimes, Iowa State Univ., Inst. Atom.Res., Dep. Metallurgica (1968).
3. Rindlhardt U. Thesis, TU Dresden (1972).
4. klein B.M., Birman J.L. Phys.Rev.Lett., 25, 1014 (1970).
5. Harrison W.A. Pseudopotentials in the Theory of Metals, W.A.Benjamin. Inc., New York (1966).
6. Shaw R.W., Jr. Phys.Rev., 174, 769 (1968).
7. Taut M., Paasch G. Preprint ES-4, TU Dresden Sektion Physik (1971).
8. Lehmann G., Rennert P., Taut M., Wonn H. phys.stat. sol., 37, K27 (1970).
9. Eschrig H., Urwank P., Wonn H. Preprint ES-3. TU Dresden, Sektion Physik (1971).

10. Parlinski K., Sudnik-Hrynkiewicz M., Bajorek A., Janik J.A., Olejarczyk W. Research Application of Nuclear Pulsed Systems, IAEA, Vienna (1967) 179.
11. В.Д. Ананьев и др. Препринт ОИЯИ, 13-4395, Дубна, 1969.
12. Bajorek A. et al. Inelastic Scattering of Neutrons, IAEA, Vienna (1966), II, 519.
13. Egelstaff P.A. Inelastic Scattering of Neutrons, IAEA, Vienna (1963), I, 65.
14. Page D.I. Neutron Inelastic Scattering, IAEA, Vienna (1968) I,325.
15. И.И. Гуревич, Л.В. Тарасов. Физика нейтронов низких энергий, Москва, 1965.
16. Sharp R.I. J.Phys. C (Solid State Phys.) 2, 421 (1969).
17. Larsson K.E., Dahlborg U., Jovic D. Inelastic Scattering of Neutrons, IAEA, Vienna (1966) II, 117.
18. Kadanov L., Martin P.C. Ann.Phys., 24, 219 (1963).
19. Vineyard G.H. Phys.Rev., 110, 999 (1958).
20. Weiss L. Thesis TU Dresden (1968).
21. М.М. Бредов, Б.А. Котов, Н.М. Окунева, В.С. Оскотский. ФТТ 9, 287 и 550 (1967).

Received by Publishing Department
on February 8, 1972.

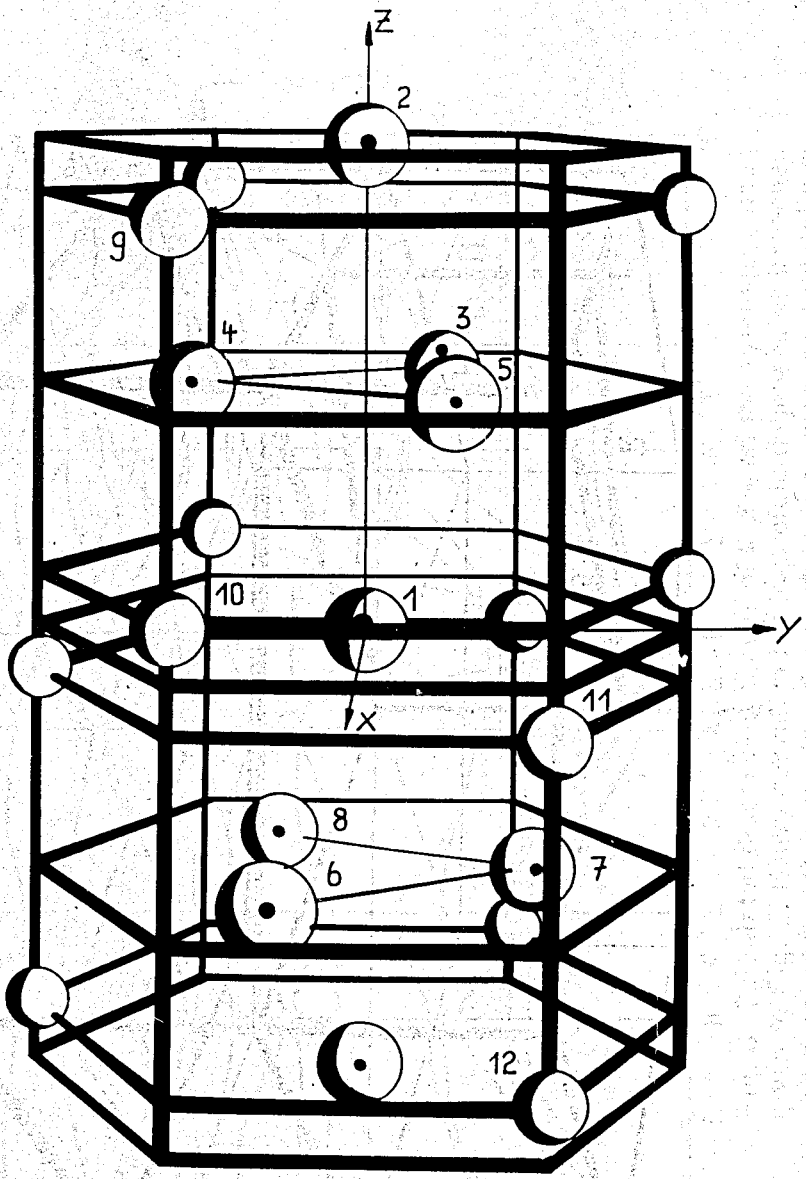

Fig. 1. Wigner Seitz cell of $MgZn_2$. Zn atoms are signed by a dot; the size of the balls corresponds to thermal neutron cross sections.

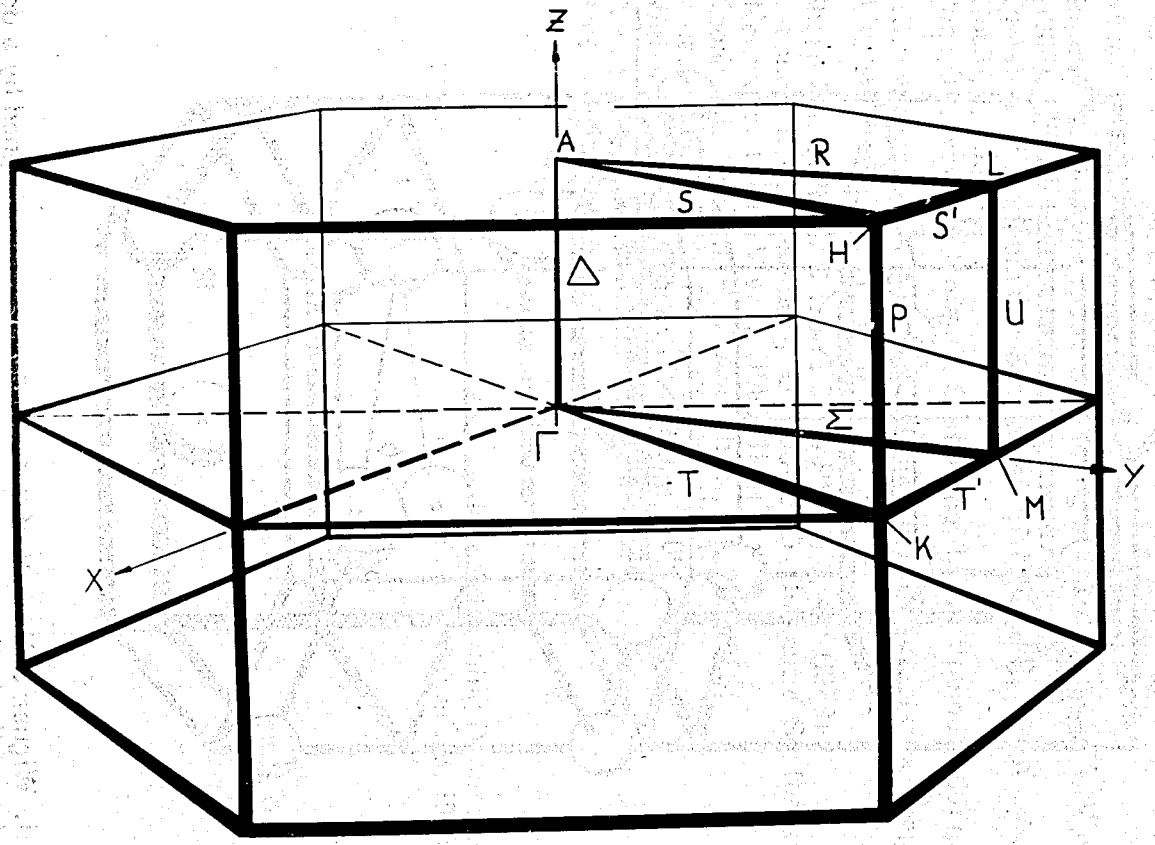

Fig. 2. Brillouin zone of the hcp structure with all symmetry lines and points.

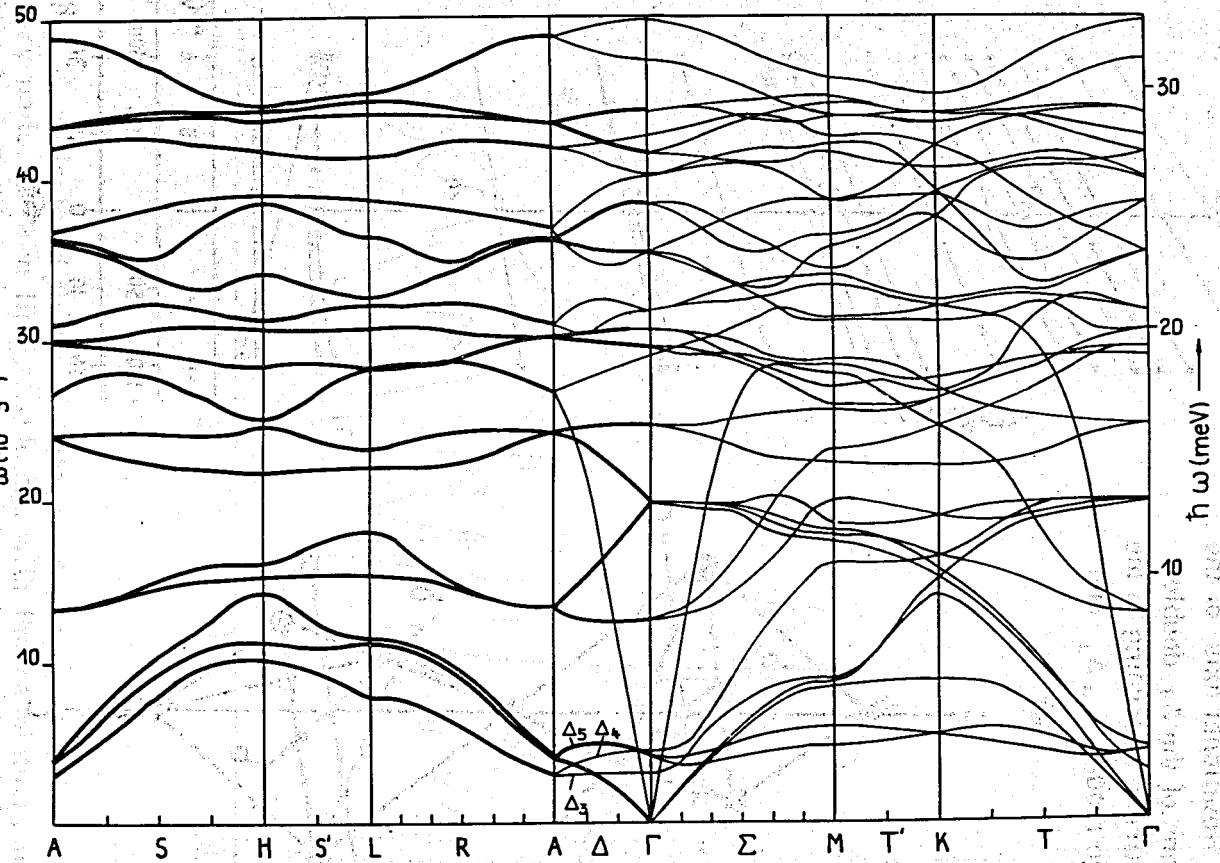

Fig. 3. Calculated dispersion curves of $MgZn_2$ on the symmetry lines given in Fig. 2. Heavy curves refer to twofold degenerates branches and point at the abscissa to wave-vectors, for which the calculations are performed. The $\Gamma-\Gamma$ part has only illustrative character; there are uncertainties at the crossing points.

Fig. 4. Rotational axis' of the vibrations of the Zn double tetrahedrons according to the cagomee modes Δ_3, Δ_4 and Δ_5.

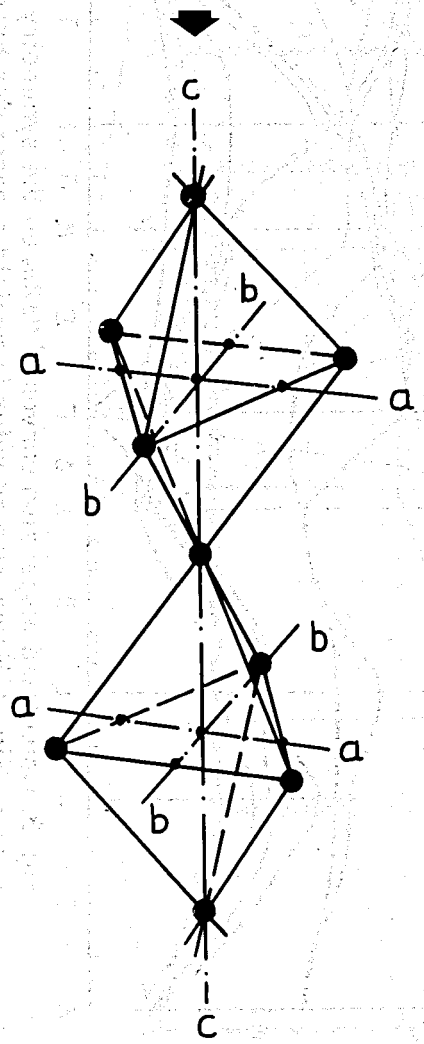

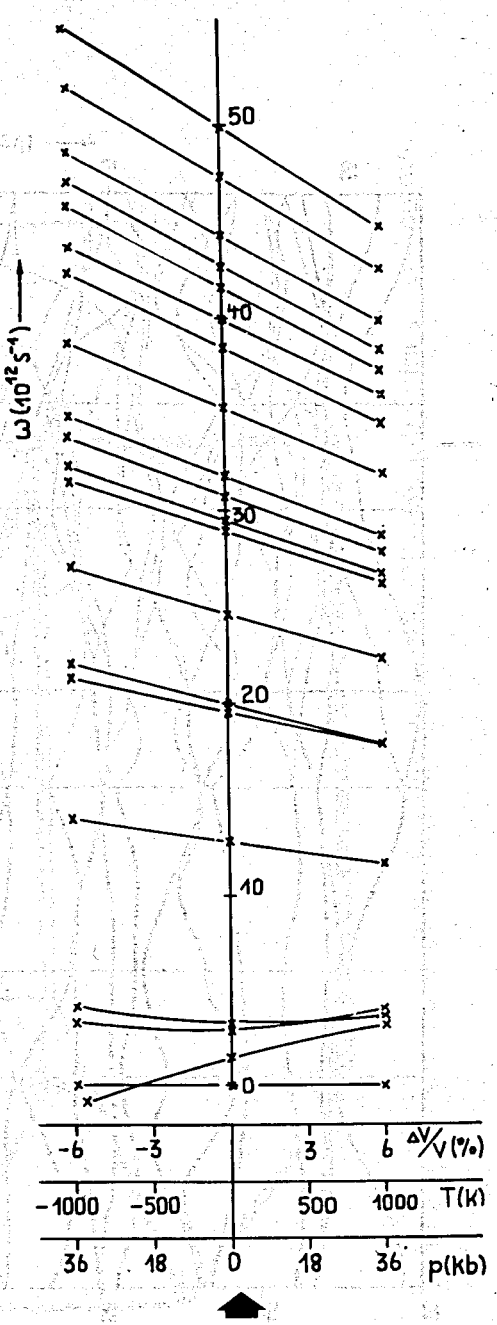

Fig. 5. Dependence of the phonon frequencies of $MgZn_2$ at point Γ from the volume expansion $(\Delta V/V)$, the temperature at zero pressure (T) and the pressure at zero temperature (p).

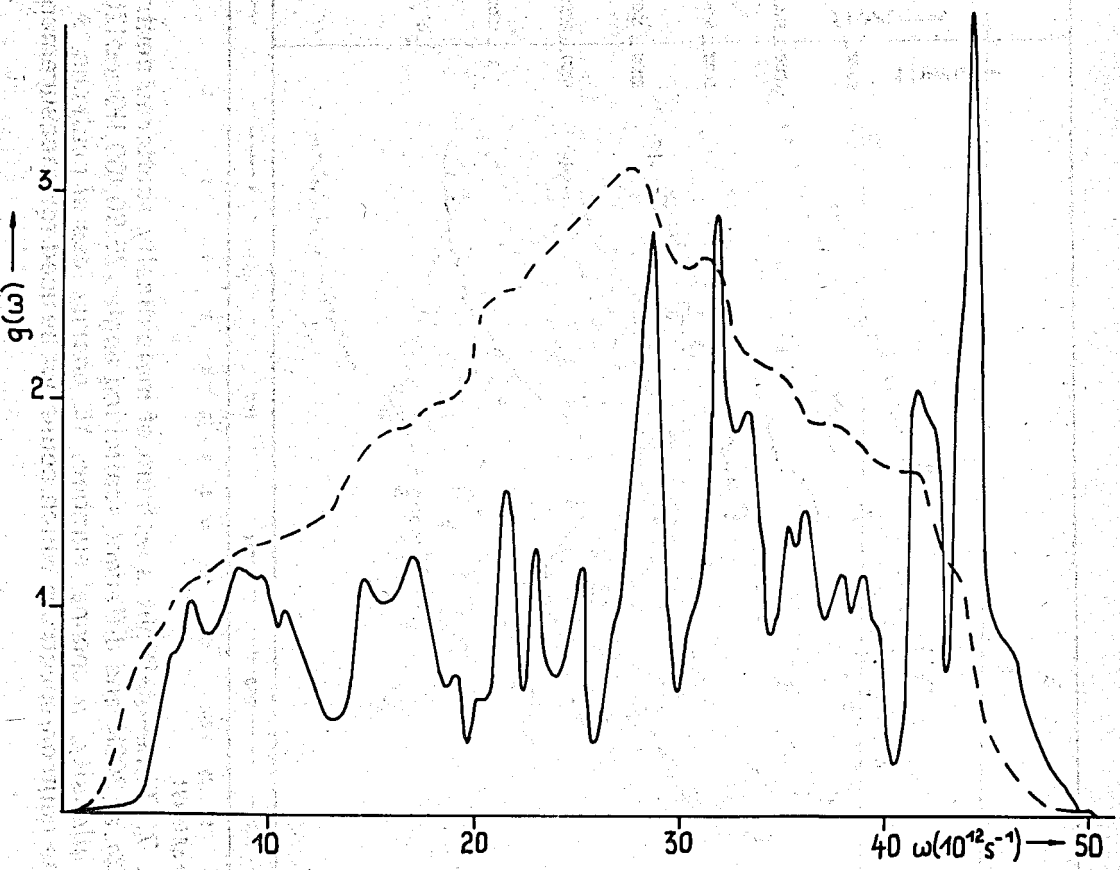

Fig. 6. Calculated phonon density of states $g(\omega)$ of $MgZn_2$ in arbitrary units. Broken line: $g(\omega)$ folded with the resolution function of the spectrometer.

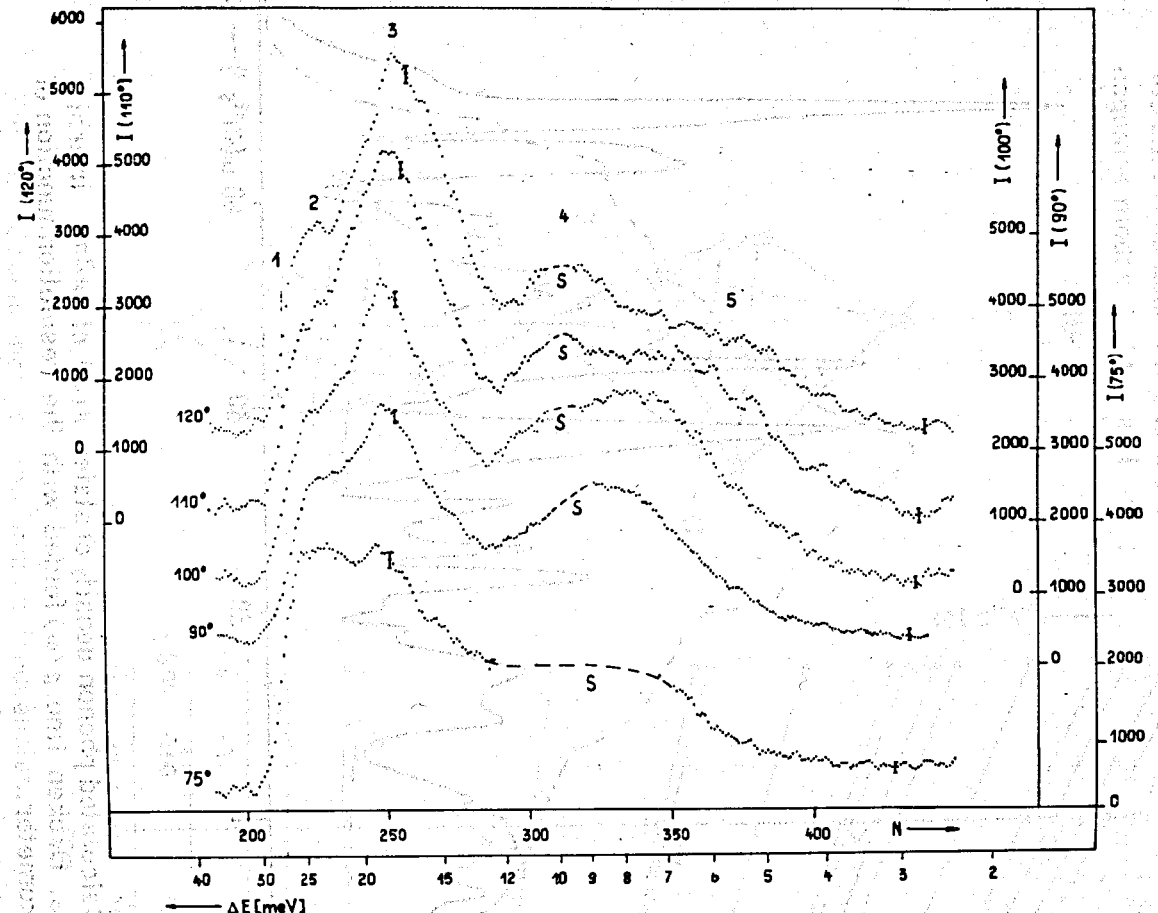

Fig. 7. Time-of-flight spectrum of inelastically scattered neutrons on $MgZn_2$ at 300K and different scattering angles 75,90,100,110 and 120 . (I intensity, N channel number, ΔE energy loss of neutrons, S part of the neutron spectrum which could not be used for measurements).

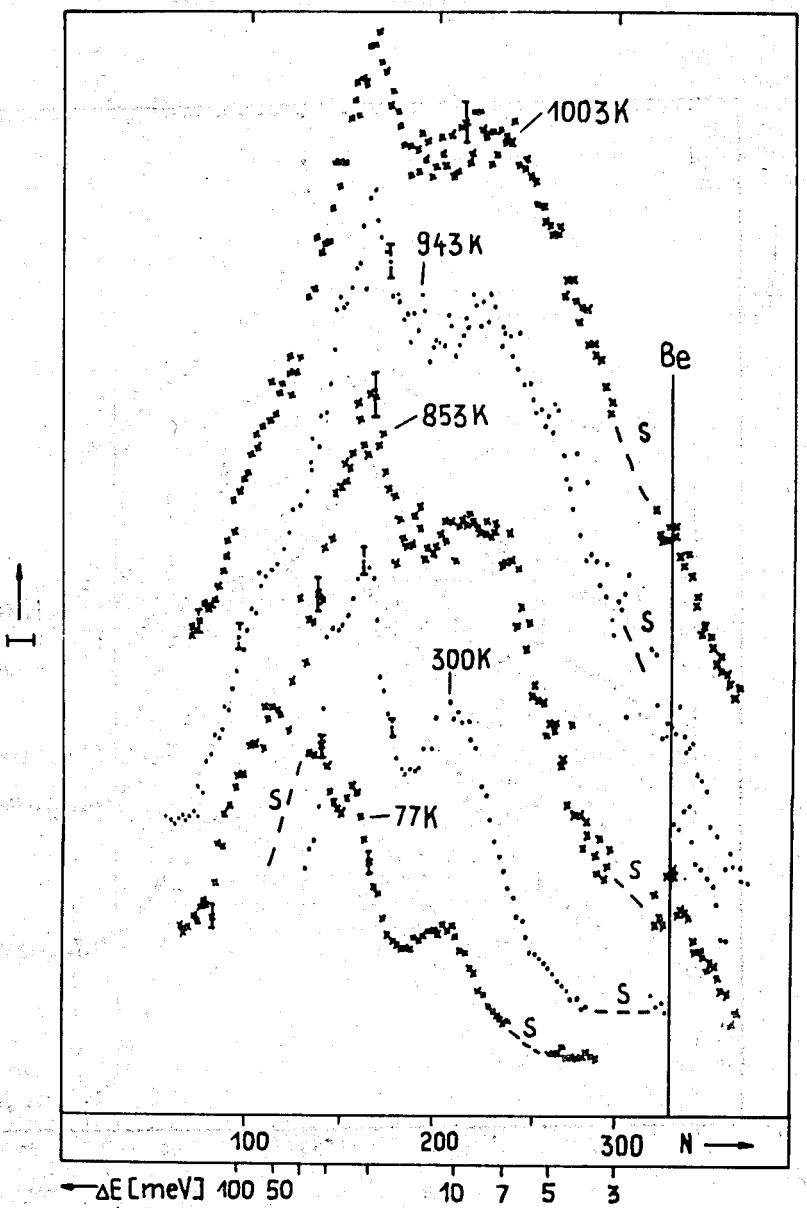

Fig. 8. Time-of-flight spectrum of inelastically scattered neutrons on $MgZn_2$ at the scattering angle 90^o for different temperatures 77, 300,853,943 and 1003K. (For details see Fig. 7 and text).

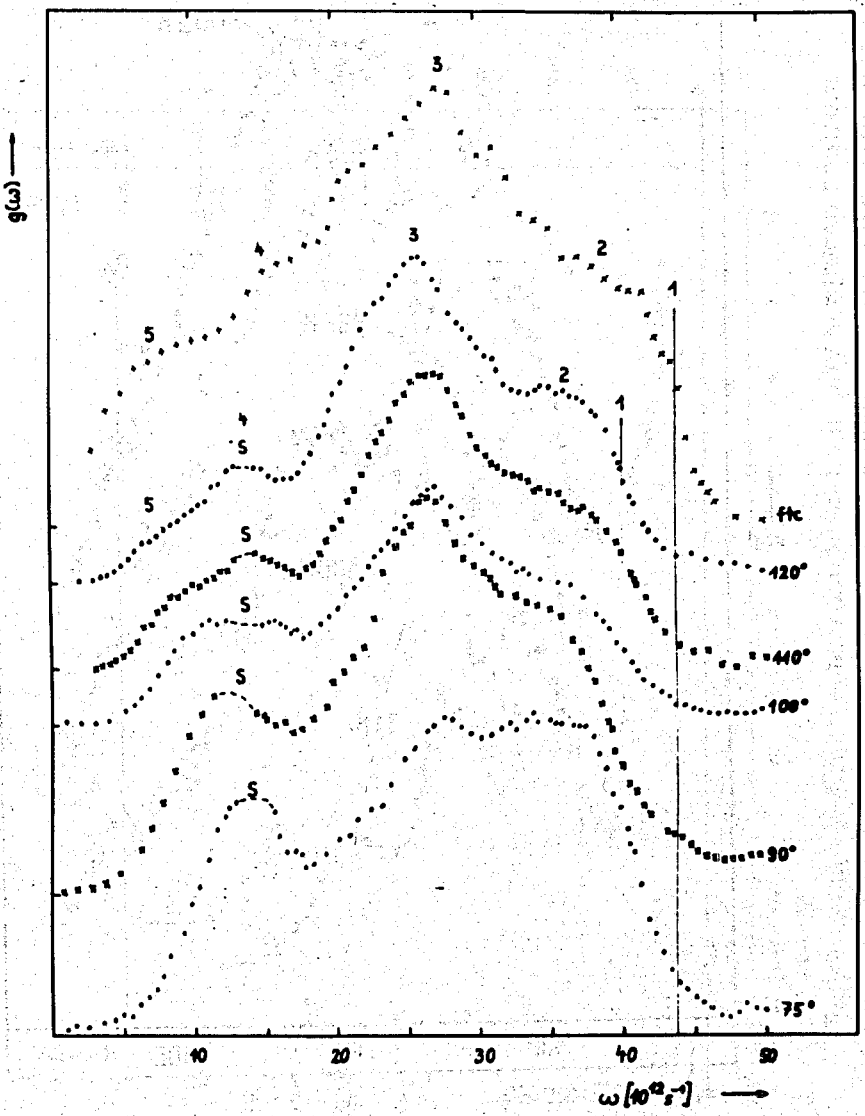

Fig. 9. Phonon density of states calculated from experimental data for different angles . (ftc folded theoretical curve from Fig. 6).